Optical and dc conductivities of cuprates: Spin fluctuation scattering in the $t - J$ model

A. A. Vladimirov,[1] D. Ihle,[2] and N. M. Plakida[1,3]
[1]*Joint Institute for Nuclear Research, 141980 Dubna, Russia*
[2]*Institut für Theoretische Physik, Universität Leipzig, D-04109, Leipzig, Germany*
[3]*Max-Planck-Institut für Physik komplexer Systeme, D-01187 Dresden, Germany*
(Received 19 December 2011; revised manuscript received 13 April 2012; published 29 June 2012)

A microscopic theory of the electrical conductivity $\sigma(\omega)$ within the $t - J$ model is developed. An exact representation for $\sigma(\omega)$ is obtained using the memory-function technique for the relaxation function in terms of the Hubbard operators, and the generalized Drude law is derived. The relaxation rate due to the decay of charge excitations into particle-hole pairs assisted by antiferromagnetic spin fluctuations is calculated in the mode-coupling approximation. Using results for the spectral function of spin excitations calculated previously, the relaxation rate and the optical and dc conductivities are calculated in a broad region of doping and temperatures. The reasonable agreement of the theory with experimental data for cuprates proves the important role of spin fluctuation scattering in the charge dynamics.

DOI: 10.1103/PhysRevB.85.224536 PACS number(s): 72.10.−d, 72.10.Bg, 78.20.Bh, 71.27.+a

I. INTRODUCTION

Studies of charge dynamics in superconducting cuprates provide valuable information concerning electron interaction with bosonic modes, which is important for elucidating the pairing mechanism in high-temperature superconductors. There is a vast literature devoted to these studies (for reviews see, e.g., Refs. 1–4). Two major scenarios have been proposed: the electron-phonon coupling and electron interaction with the antiferromagnetic (AF) spin fluctuations. Angle-resolved photoemission spectroscopy (ARPES) points to an important role of spin fluctuations in a renormalization of the single-electron excitation spectrum (see, e.g., Ref. 5 and references therein), which is supported by measurements of the infrared (IR) absorption in a wide region of temperatures and doping (see, e.g., Refs. 6–8 and references therein). The main argument against the spin fluctuation pairing mechanism, a weak intensity of spin fluctuations at the optimal doping seen in inelastic magnetic neutron scattering experiments,[9] was dismissed in recent resonant inelastic x-ray scattering.[10] In a large family of cuprates, AF paramagnon excitations with dispersions and spectral weights similar to those of magnons in undoped cuprates were found. However, a decisive role of the electron-phonon interaction (EPI) has been claimed in a number of theoretical studies (for a review, see Ref. 11).

The optical conductivity (OC) $\sigma(\omega)$ of cuprates reveals a complicated evolution with doping and temperature. The undoped parent compounds are AF insulators, where the OC exhibits a peak at the charge-transfer energy $\omega \lesssim 1.8$ eV. Under doping, the insulator-to-metal transition occurs when the charge-transfer gap is filled up with states and the spectral weight is transferred to the lower energy, the Drude peak at $\omega \to 0$ with a width $\omega \lesssim 600$ cm^{-1}, and a broad mid-infrared (MIR) band at higher energies $\omega \lesssim 5000$ cm^{-1}. With increasing hole concentration, the MIR absorption shifts to lower energies and merges with the Drude contribution (see, e.g., Refs. 12–16). The Drude peak significantly narrows with decreasing temperature and is attributed to the relaxation of coherent quasiparticles, while the origin of the temperature-independent MIR contribution is still under discussion. In Ref. 17, the metal-to-insulator transition (MIT) was studied by measuring the OC for the underdoped Bi-based and YBCO-based compounds for hole concentrations from $\delta = 0.12$ to 0.015. With decreasing hole concentration, the Drude peak at low temperatures transforms into a far-infrared (FIR) band at energies $\omega \gtrsim 200$ cm^{-1}, which acquires a gap at the MIT for hole doping $\delta \lesssim 0.07$. Note that the onset of the metallic phase occurs at a doping much higher than $\delta \simeq 0.02$ at which the AF long-range order (LRO) vanishes.[18]

It is generally believed that superconducting cuprates are doped Mott-Hubbard (charge-transfer)[19] insulators, where the insulating phase of the undoped parent compounds appears due to a strong Coulomb repulsion, Hubbard $U > U_{c2}$, where the critical value U_{c2} for the MIT is larger than the electronic bandwidth W (see, e.g., Ref. 20). In this case, the AF LRO in the undoped compounds originates from the strong AF exchange interaction characteristic for Hubbard systems. However, it is also possible to explain the insulating phase as caused by the AF energy gap induced by the AF LRO where the Coulomb interaction plays a secondary role. In recent publications, this problem was discussed by analyzing the OC for typical electron-doped $Nd_{2-x}Ce_xCuO_4$ (NCCO) and hole-doped $La_{2-x}Sr_xCuO_4$ (LSCO) compounds. In Ref. 21, the OC was calculated for the Hubbard model in the paramagnetic and the AF phases. Using the dynamical mean-field theory (DMFT),[22] the optical spectral weight [given by the restricted sum rule with the integration over energy in Eq. (3) up to $\Omega = 0.8$ eV] was calculated. Comparing the doping dependence of the theoretical and measured spectral weights for the NCCO, LSCO, and other cuprate compounds, it was found that, in the paramagnetic phase, the fitted U is smaller than the critical value $U_{c2} \sim 1.5$ W for yielding the Mott-Hubbard insulating phase. At the same time, the AF phase provides the insulating state for the undoped system at the fitted U. So, it was concluded that antiferromagnetism is essential in producing the insulating state.

A different conclusion concerning the hole-doped cuprates was obtained in Refs. 23 and 24. The OC was calculated for a realistic three-band p-d model for NCCO and LSCO using the local density approximation combined with the DMFT.[25] It

was found that, whereas for the electron-doped NCCO the AF interaction is necessary to yield the insulating undoped state, the hole-doped LSCO belongs to the Mott-Hubbard system, where the insulating state is due to strong electron correlations but not to the AF interaction. However, in the DMFT, the short-range AF correlations are neglected. As shown in Ref. 26, by taking them into account, we find a much narrower Hubbard band $\widetilde{W}$, which leads to a lower critical parameter U_{c2} that may put the electron-doped compounds also into the class of Mott-Hubbard insulators. Therefore, for a more accurate estimation of U_{c2}, the cluster DMFT (Ref. 27) should be used. By this method, the OC was calculated in the $t-J$ model in Ref. 28. The results reproduced quite well the delicate changes of the spectral weight transfer at the transition to the superconducting phase observed in experiments (see, e.g., Refs. 29 and 30 and references therein). This proves that the $t-J$ model captures the essential physics of the low-energy excitations in cuprates.

In the limit of strong correlations, extensive numerical studies of the OC within the Hubbard model and $t-J$ model for finite systems have been carried out. Earlier results are reported in Refs. 31–35. Due to a small size of the clusters, only one- or two-hole motion was considered. In that case, the Drude peak can not be resolved, and its intensity versus doping was studied by calculations of the kinetic energy [see Eq. (20)]. Several peaks found in the OC in the MIR region may be related to local spin excitations at $\omega \simeq 2J$ and to string excitations at higher energies. This observation was confirmed in analytical studies of the charge correlations in a weakly doped $t-J$ model using the cumulant expansion within the Zwanzig-Mori projection technique.[36] The peaks found in the OC in the energy region $\omega \simeq 2J$ were assigned to excitations due to internal degrees of freedom of the spin-bag quasiparticles.

In several studies, an important role of the EPI resulting in polaronic effects was stressed. However, contradicting explanations were proposed for the two absorption bands observed in the MIR region, one at a lower energy near the FIR region and another at higher energies. In Ref. 37, the OC of one hole in the Holstein $t-J$ model using the DMFT was calculated. It was shown that the IR absorption is characterized by the coexistence of a magnon peak at low energy and a broad polaronic band at higher energy. The two absorption bands were explained in Ref. 38 by the coupling of a hole to two kinds of bosonic excitations. The lower energy peak at $\omega \simeq 1000$ cm^{-1} was ascribed to the phonon sideband, while the higher-energy peak at $\omega \simeq 4600$ cm^{-1} was considered as the magnon sideband of the lower peak. As discussed in Ref. 39, the two-peak structure in the MIR region may be explained by the coupling of a doped hole to magnetic excitations. The low-energy peak represents the local magnetic excitation, attached to the hole, while the higher-frequency peak corresponds to the MIR band that originates from coupling to spin-wave excitations, broadened and renormalized by phonon excitations. Thus, the studies of the Holstein $t-J$ model suggest that the complicated absorption structure experimentally found in the MIR region is caused by magnetic excitations, which are coupled to phonons via doped holes.

In analytical studies, the OC is frequently evaluated within the simple electron-hole (bubble) diagram approximation for the current-current correlation function proposed by Allen.[40] The finite-temperature version of the Allen approximation was derived in Ref. 41. This method was used in studies of the optical IR data within electron-phonon models (see Ref. 11 and references therein) and spin-fermion models (see, e.g., Refs. 42 and 43 and references therein).

A general approach based on the Mori memory-function method[44] for the calculation of the current-current relaxation function was proposed in Ref. 45. In this method, the transport relaxation rate is expressed directly in terms of the force-force relaxation function, which can be further evaluated by perturbation theory with a proper consideration of the wave-vector dependence of the transport vertex. In particular, in Ref. 46, the memory-function method was used to calculate the OC in the limit of strong electron correlations within the Emery model for CuO_2 plane. The relaxation rate for electrons scattered by AF spin fluctuations was calculated in a fair agreement with experiments. In Ref. 47, by taking into account only the incoherent part of the electronic spectrum, a scaling expression for the frequency dependence of the relaxation rate and the conductivity in the $t-J$ model was obtained.

Electron interactions with bosonic modes can be revealed in the low-energy part of the OC and dc conductivity. To shed more light on the scattering mechanism in cuprates, in this paper we calculate the optical and dc conductivities within the $t-J$ model. The main goal of this work is to demonstrate that AF spin fluctuation scattering is the essential mechanism of the low-energy charge dynamics of underdoped and optimally doped cuprates.

Using the memory-function method, we derive an equation for the relaxation rate which is determined by the kinematic interaction for the Hubbard operators and depends only on the parameters of the $t-J$ model: the hopping parameters and the AF exchange coupling. The relaxation rate is calculated by taking into account electron scattering by spin fluctuations, which are described by the spin-excitation spectral function calculated in our previous works.[48,49] Therefore, we are able to consider effects of spin excitations on the charge dynamics within a microscopic theory without fitting parameters. In our approach, we obtain a reasonable agreement with experiments for the relaxation rate, the optical conductivity, and the resistivity in broad regions of temperature and doping, in particular, in the underdoped region with a strong AF short-range order (SRO).

In Sec. II, we formulate a general theory of the optical conductivity within the memory-function formalism. The application of this theory to the $t-J$ model is given in Sec. III. Numerical results and discussion are presented in Sec. IV. In Sec. V, we summarize our results.

II. MEMORY-FUNCTION THEORY

In the linear response theory of Kubo,[50] the frequency-dependent conductivity is defined by the current-current relaxation function

$$\sigma_{xx}(\omega) = \frac{i}{V}\langle\langle J_x|J_x\rangle\rangle_\omega = \frac{1}{V}\int_0^\infty dt\, e^{i\omega t}(J_x(t), J_x), \qquad (1)$$

where V is the volume of the system. Here, the Kubo–Mori scalar product

$$(A(t),B)=\int_0^\beta d\lambda\langle A(t-i\lambda)B\rangle \tag{2}$$

for the operators in the Heisenberg representation $A(t)=\exp(iHt)A\exp(-iHt)$ is introduced. $\langle AB\rangle$ denotes the equilibrium statistical average for a system with the Hamiltonian H (here $\beta=1/T,\hbar=k_B=1$). The real part of the conductivity (1) obeys the sum rule

$$\int_0^\infty d\omega\,\mathrm{Re}\sigma_{xx}(\omega)=\frac{\pi}{2V}\chi_0=\frac{i\pi}{2V}\langle[J_x,P_x]\rangle. \tag{3}$$

Here, $P_x=e\sum_i R_i^x N_i$ is the polarization operator. R_i^x is the x component of the lattice vector pointing to site i, e is the electron charge, and N_i is the number operator. The current operator is defined by the time derivative of the polarization operator: $J_x(t)=dP_x(t)/dt\equiv\dot{P}_x(t)=-i[P_x,H]$. The static current-current susceptibility $\chi_0=(J_x,J_x)$ is related to the effective number of charge carriers participating in the absorption

$$N_{\mathrm{eff}}=\frac{2mv_0}{\pi e^2}\int_0^\infty d\omega\,\mathrm{Re}\sigma_{xx}(\omega)=\frac{m}{e^2N}\chi_0\,, \tag{4}$$

where $v_0=V/N$ is the unit-cell volume and m is the free-electron mass. The sum rule (3) is frequently written in terms of the plasma frequency ω_{pl} defined by $\omega_{\mathrm{pl}}^2=4\pi\chi_0/V=\omega_{0,\mathrm{pl}}^2N_{\mathrm{eff}}$, where $\omega_{0,\mathrm{pl}}^2=4\pi Ne^2/mV$.

To calculate the conductivity (1), it is convenient to employ the memory-function approach of Mori[44] by introducing the memory function $M(\omega)$ for the relaxation function[45]

$$\Phi(\omega)\equiv(\!(J_x|J_x)\!)_\omega=\frac{\chi_0}{\omega+M(\omega)}. \tag{5}$$

From the equations of motion for the relaxation function $\Phi(t-t')=(\!(J_x(t)|J_x(t'))\!)$, the memory function is determined by (see Appendix A)

$$M(\omega)=(\!(F_x|F_x)\!)_\omega^{(\mathrm{proper})}(1/\chi_0), \tag{6}$$

where $F_x=i\dot{J}_x=[J_x,H]$ is the force operator. The definition of the memory function (6) as the "proper" part of the force-force relaxation function is equivalent to the introduction of the projected Liouvillian superoperator for the memory function in the original Mori technique.[44]

Using Eq. (5), the frequency-dependent conductivity (1) can be written in the form of the generalized Drude law

$$\sigma_{xx}(\omega)\equiv\sigma(\omega)=\frac{\omega_{\mathrm{pl}}^2}{4\pi}\,\frac{m}{\widetilde{m}(\omega)}\,\frac{1}{\widetilde{\Gamma}(\omega)-i\omega}, \tag{7}$$

where the effective optical mass and the relaxation rate are given by

$$\frac{\widetilde{m}(\omega)}{m}=1+\lambda(\omega),\quad \widetilde{\Gamma}(\omega)=\frac{\Gamma(\omega)}{1+\lambda(\omega)}, \tag{8}$$

$$\lambda(\omega)=M'(\omega)/\omega,\quad \Gamma(\omega)=M''(\omega). \tag{9}$$

Here, the real and imaginary parts of the retarded memory function $M(\omega+i0^+)=M'(\omega)+iM''(\omega)$ are introduced. They are coupled by the dispersion relation

$$M'(\omega)=\frac{1}{\pi}\int_{-\infty}^{\infty}d\omega'\,\frac{M''(\omega')}{\omega'-\omega}. \tag{10}$$

Both the real and imaginary parts of the memory function can be directly related to experimental data for the inverse conductivity (7) (Ref. 2):

$$\Gamma(\omega)=\frac{\omega_{\mathrm{pl}}^2}{4\pi}\,\mathrm{Re}\frac{1}{\sigma(\omega)},\quad 1+\lambda(\omega)=-\frac{\omega_{\mathrm{pl}}^2}{4\pi\omega}\,\mathrm{Im}\frac{1}{\sigma(\omega)}. \tag{11}$$

In the following, we calculate these functions for the $t-J$ model.

III. RELAXATION RATE

We consider the $t-J$ model on the square lattice, which in the conventional notation reads as[51,52]

$$H=H_t+H_J=-\sum_{i\neq j,\sigma}t_{ij}\tilde{a}_{i\sigma}^+\tilde{a}_{j\sigma}-\mu\sum_i N_i +\frac{1}{2}\sum_{i\neq j,\sigma}J_{ij}\left(\mathbf{S}_i\mathbf{S}_j-\frac{1}{4}N_iN_j\right), \tag{12}$$

where t_{ij} is the hopping integral and J_{ij} is the AF exchange interaction. Here, $\tilde{a}_{i\sigma}^+=a_{i\sigma}^+(1-n_{i\bar{\sigma}})$ is the projected electron operator with spin $\sigma/2=\pm1/2$ ($\bar{\sigma}=-\sigma$) on the lattice site i, $N_i=\sum_\sigma\tilde{a}_{i\sigma}^+\tilde{a}_{i\sigma}$ is the number operator, and $S_i^\alpha=(1/2)\sum_{s,s'}\tilde{a}_{is}^+\sigma_{s,s'}^\alpha\tilde{a}_{is'}$ is the α component of the spin operator ($\sigma_{s,s'}^\alpha$ are Pauli matrices). The chemical potential μ is determined from the equation for the average electron occupation number $\langle N_i\rangle=1-\delta$, where δ is the hole concentration.

To take into account the projected character of electron operators, we employ the Hubbard operator (HO) technique.[53,54] The HO $X_i^{\alpha\beta}=|i,\alpha\rangle\langle i,\beta|$ describes the transition from the state $|i,\beta\rangle$ to the state $|i,\alpha\rangle$ at the site i, where α and β denote three possible states: an empty state ($\alpha,\beta=0$) and a singly occupied state ($\alpha,\beta=\sigma$). The completeness relation $X_i^{00}+\sum_\sigma X_i^{\sigma\sigma}=1$ rigorously preserves the constraint of no double occupancy of any lattice site. From the multiplication rule $X_i^{\alpha\beta}X_i^{\gamma\delta}=\delta_{\beta\gamma}X_i^{\alpha\delta}$ follow the commutation relations for the HOs:

$$\left[X_i^{\alpha\beta},X_j^{\gamma\delta}\right]_\pm=\delta_{ij}\left(\delta_{\beta\gamma}X_i^{\alpha\delta}\pm\delta_{\delta\alpha}X_i^{\gamma\beta}\right). \tag{13}$$

The upper sign refers to the Fermi-type operators creating ($X_i^{\sigma0}$) or annihilating ($X_j^{0\sigma}$) electrons, while the lower sign refers to the Bose-type operators, such as the number or spin operators:

$$N_i=\sum_\sigma X_i^{\sigma\sigma},\quad S_i^z=\frac{1}{2}\sum_\sigma\sigma X_i^{\sigma\sigma},\quad S_i^\sigma=X_i^{\sigma\bar{\sigma}}. \tag{14}$$

The commutation relations result in *the kinematic interaction* for HOs [see Eq. (B3)]. Note that the term "kinematic interaction" was introduced by Dyson[55] for spin operators.

Using the HO representation for $\tilde{a}_{i\sigma}^+=X_i^{\sigma0}$, $\tilde{a}_{j\sigma}=X_j^{0\sigma}$, and Eq. (14), we write the Hamiltonian (12) in the

form

$$H = -\sum_{i\neq j,\sigma} t_{ij}\, X_i^{\sigma 0} X_j^{0\sigma} - \mu \sum_{i\sigma} X_i^{\sigma\sigma} + \frac{1}{4}\sum_{i\neq j,\sigma} J_{ij}\left(X_i^{\sigma\bar{\sigma}} X_j^{\bar{\sigma}\sigma} - X_i^{\sigma\sigma} X_j^{\bar{\sigma}\bar{\sigma}}\right). \quad (15)$$

The relaxation rate $\Gamma(\omega) = M''(\omega)$ is calculated by Eq. (6) in the mode-coupling approximation (MCA) as described in Appendix B. In this approximation, we obtain

$$\Gamma(\omega) = \frac{(e^{\beta\omega}-1)}{\chi_0\,\omega}\frac{2\pi\, e^2}{N}\sum_{\mathbf{k},\mathbf{q}}\int\!\!\int\!\!\int_{-\infty}^{\infty} d\omega_1 d\omega_2 d\omega_3 \times n(\omega_1)[1-n(\omega_2)]N(\omega_3)\,\delta(\omega_2-\omega_1-\omega_3+\omega) \times g_x^2(\mathbf{k},\mathbf{k}-\mathbf{q})\chi''_{cs}(\mathbf{q},\omega_3)A(\mathbf{k},\omega_1)A(\mathbf{k}-\mathbf{q},\omega_2), \quad (16)$$

where $n(\omega) = (\exp\beta\omega + 1)^{-1}$ and $N(\omega) = (\exp\beta\omega - 1)^{-1}$. The momentum-dependent (transport) vertex is given by

$$g_x(\mathbf{k},\mathbf{k}-\mathbf{q}) = v_x(\mathbf{k})\,t(\mathbf{k}-\mathbf{q}) - v_x(\mathbf{k}-\mathbf{q})\,t(\mathbf{k}) - J(\mathbf{q})/2\,[v_x(\mathbf{k}) - v_x(\mathbf{k}-\mathbf{q})], \quad (17)$$

where $t(\mathbf{k})$ and $J(\mathbf{q})$ are the Fourier transforms of the hopping integral and the exchange interaction, and $v_x(\mathbf{k}) = -\partial t(\mathbf{k})/\partial k_x$ is the electron velocity (see Appendix B). The spectral function for the charge-spin excitations $\chi''_{cs}(\mathbf{q},\omega) = (1/\pi)\mathrm{Im}\,\chi_{cs}(\mathbf{q},\omega)$ is defined by the corresponding commutator Green's functions (GFs)

$$\chi_{cs}(\mathbf{q},\omega) = -(1/4)\langle\langle N_{\mathbf{q}}|N_{-\mathbf{q}}\rangle\rangle_\omega - \langle\langle \mathbf{S}_{\mathbf{q}}|\mathbf{S}_{-\mathbf{q}}\rangle\rangle_\omega, \quad (18)$$

where we used Zubarev's notation[56] for the retarded two-time GFs. The spectral function of electronic excitations is defined by the imaginary part of the anticommutator electronic GF:

$$A(\mathbf{k},\omega) = -(1/\pi)\,\mathrm{Im}\left\langle\!\left\langle X_{\mathbf{k}}^{0\sigma}|X_{\mathbf{k}}^{\sigma 0}\right\rangle\!\right\rangle_\omega. \quad (19)$$

The static current-current susceptibility χ_0 is connected with the effective number of charge carriers (4), which for the $t-J$ model reads as

$$N_{\mathrm{eff}} = \frac{m}{N}\sum_{i,j,\sigma}\left(R_i^x - R_j^x\right)^2 t_{ij}\left\langle X_i^{\sigma 0} X_j^{0\sigma}\right\rangle = -\frac{m}{N}\sum_{\mathbf{k},\sigma}\frac{\partial^2 t(\mathbf{k})}{\partial k_x^2}\left\langle X_{\mathbf{k}}^{\sigma 0} X_{\mathbf{k}}^{0\sigma}\right\rangle. \quad (20)$$

For the $t-J$ model with the nearest-neighbor hopping only, $(R_i^x - R_j^x)^2 = a^2$, where a is the lattice parameter, the effective number of carriers is related to the averaged kinetic energy $N_{\mathrm{eff}} = (a^2 m/N)\langle -H_t\rangle$. This relation is often used in the calculation of the charge stiffness (Drude weight) in finite-cluster studies (see, e.g., Refs. 31 and 32).

IV. RESULTS AND DISCUSSION

A. Spectral functions

In numerical calculations, we have to use models for the charge-spin susceptibility (18) and the one-electron spectral function (19). The spin-excitation contribution in Eq. (18) is described by the spectral function $\chi''_s(\mathbf{q},\omega) = (3/2)\chi''_\pm(\mathbf{q},\omega)$, where $\chi''_\pm(\mathbf{q},\omega) = -(1/\pi)\mathrm{Im}\,\langle\langle S_{\mathbf{q}}^+|S_{-\mathbf{q}}^-\rangle\rangle_\omega$. For the latter, we use the function calculated in Ref. 48 for the $t-J$ model,

$$\chi''_\pm(\mathbf{q},\omega) = \frac{-\omega\,\Sigma_s''(\mathbf{q})\,(m(\mathbf{q})/\pi)}{\left[\omega^2 - \omega_{\mathbf{q}}^2 - \omega\,\Sigma_s'(\mathbf{q},\omega)\right]^2 + [\omega\,\Sigma_s''(\mathbf{q})]^2}. \quad (21)$$

Here, the spectrum of spin excitations in the generalized mean-field approximation $\omega_{\mathbf{q}}$ determines the static spin susceptibility $\chi_{\mathbf{q}} = m(\mathbf{q})/\omega_{\mathbf{q}}^2$ with $m(\mathbf{q}) = \langle[i\dot{S}_{\mathbf{q}}^+, S_{-\mathbf{q}}^-]\rangle$, where $i\dot{S}_{\mathbf{q}}^+ = [S_{\mathbf{q}}^+, H]$. The self-energy $\Sigma_s(\mathbf{q},\omega) = \Sigma_s'(\mathbf{q},\omega) + i\,\Sigma_s''(\mathbf{q},\omega)$, where $\Sigma_s'(\mathbf{q},\omega)$ and $\Sigma_s''(\mathbf{q},\omega)$ are the real and the imaginary parts, respectively, is determined by the many-particle relaxation function $\Sigma_s(\mathbf{q},\omega) = [1/m(\mathbf{q})]\langle\langle -\ddot{S}_{\mathbf{q}}^+|-\ddot{S}_{-\mathbf{q}}^-\rangle\rangle_\omega^{\mathrm{proper}}$ calculated in MCA (see Refs. 48 and 49). Taking into account that the main contribution to the relaxation rate (16) from the spectral function (21) is given by frequencies close to the renormalized spin-excitation frequency $\widetilde{\omega}_{\mathbf{q}} = [\omega_{\mathbf{q}}^2 + \widetilde{\omega}_{\mathbf{q}}\,\Sigma_s'(\mathbf{q},\widetilde{\omega}_{\mathbf{q}})]^{1/2}$, we approximate the damping of spin excitations by the function $\Sigma_s''(\mathbf{q}) = \Sigma_s''(\mathbf{q},\omega = \widetilde{\omega}_{\mathbf{q}})$.

To calculate the contribution to the relaxation rate (16) from charge (density) excitations in Eq. (18), we use the spectral function calculated in Ref. 57 for the $t-J$ model. Our results show that charge excitations give the main contribution in the region of high energies, $\omega \sim 3t$, which, however, is several times weaker than the spin-excitation contribution and, therefore, can be safely ignored. The different energy scales for spin excitations $\omega \sim J$ and density excitations $\omega \sim t$ were also found in an exact diagonalization study of the $t-J$ model.[34]

The self-consistent solution of the system of equations for the spectral function (19) and the single-electron self-energy in Ref. 58 has shown that close to the Fermi energy, there appear well-defined quasiparticle excitations. This result permits to approximate the spectral function by the expression

$$A(\mathbf{k},\omega) = Q\,\delta(\omega - \tilde{\varepsilon}_{\mathbf{k}}), \quad (22)$$

where $Q = 1 - n/2$ is the spectral weight for electronic excitations in the $t-J$ model. To model a realistic electronic spectrum which crosses the AF Brillouin zone (BZ), as observed in ARPES experiments (see, e.g., Ref. 59), we consider the model dispersion

$$\tilde{\varepsilon}_{\mathbf{k}} = -4Q[t\,\alpha_1\gamma(\mathbf{k}) + t'\alpha_2\,\gamma'(\mathbf{k}) + t''\alpha_2\,\gamma''(\mathbf{k})] - \mu, \quad (23)$$

where t and $t' = 0.1t, t'' = 0.2t$ are the hopping parameters for the nearest and further-distant neighbors, respectively, and $\gamma(\mathbf{k}) = (1/2)(\cos ak_x + \cos ak_y)$, $\gamma'(\mathbf{k}) = \cos ak_x \cos ak_y$, and $\gamma''(\mathbf{k}) = (1/2)(\cos 2ak_x + \cos 2ak_y)$. The kinematic interaction for the HOs results in a renormalization of the spectrum (23) determined by the parameters $\alpha_1 = [1 + C_1/Q^2]$ and $\alpha_2 = [1 + C_2/Q^2]$, where $C_1 = \langle\mathbf{S_i}\mathbf{S}_{\mathbf{i}\pm\mathbf{a}_x/\mathbf{a}_y}\rangle$ and $C_2 = \langle\mathbf{S_i}\mathbf{S}_{\mathbf{i}\pm\mathbf{a}_x\pm\mathbf{a}_y}\rangle \approx \langle\mathbf{S_i}\mathbf{S}_{\mathbf{i}\pm 2\mathbf{a}_x/2\mathbf{a}_y}\rangle$ are the spin correlation functions for the nearest and the second neighbors, respectively (see Ref. 58). With increasing doping, the effective bandwidth $\widetilde{W}$ of the dispersion (23) increases due to the decrease of AF SRO described by the doping dependence of the spin correlation functions in the renormalization parameters α_1, α_2. In particular, for $\delta = 0.09\,(0.2)$ at $T = 0$ we have $\widetilde{W} = 1.14\,t\,(2.78\,t)$ in comparison with the unrenormalized bandwidth $W = 8\,t\,Q = 4.36\,t\,(4.8\,t)$.

The Fermi surface (FS) determined by the equation $\tilde{\varepsilon}_{\mathbf{k}_\mathrm{F}} = 0$ is shown in Fig. 1 for various doping. The renormalization of the spectrum induced by the AF SRO provides a FS with hole

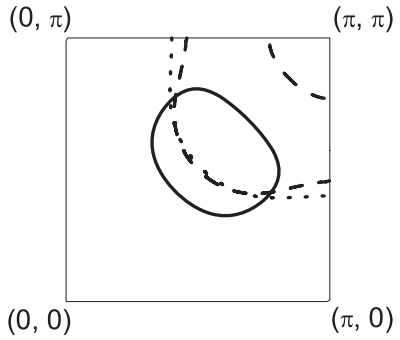

FIG. 1. Fermi surface at $\delta = 0.09$ (solid line), 0.16 (dashed line), and 0.2 (dots).

pockets at low doping, which is equivalent to a pseudogap in the $(\pm\pi,0)$ and $(0,\pm\pi)$ regions of the BZ. In the study of the electronic spectrum and the FS of cuprates, a more accurate calculation of the spectral function (22) including the self-energy contribution was performed as reported in Refs. 58 and 60 for the $t-J$ model and in Ref. 26 for the two-subband Hubbard model. In particular, in Ref. 26 the spectral function on the FS close to the (π,π) point of the BZ has a weak intensity resulting in an arc-type FS as observed in ARPES experiments. By taking into account that the spectral function of spin excitations (21) is peaked at the AF wave vector $\mathbf{Q} = (\pi,\pi)$ and is very broad in other parts of the BZ (see Ref. 49), in the calculation of the relaxation rate (16), only those parts of the FS are important which are coupled by the AF wave vector $\mathbf{Q}$. Therefore, the parts of the FS in Fig. 1 far away from the AF BZ, in particular the back side of the hole pocket near $(\pi/2,\pi/2)$ of the BZ, give small contributions at the integration over the BZ in Eq. (16). This reasoning justifies the quasiparticle approximation (22) used in the calculation of the relaxation rate.

The effective number of charge carriers (20) is convenient to write in the form

$$N_{\rm eff}(\delta) = \eta K(\delta) = \eta \frac{Q}{N} \sum_{\mathbf{k},\sigma} n(\tilde{\varepsilon}_{\mathbf{k}}) [\cos(ak_x) + 2(t'/t)\cos(ak_x)\cos(ak_y) + 4(t''/t)\cos(2ak_x)]. \quad (24)$$

For the spectral function (22), the average electron occupation number is given by $\langle X^{\sigma 0}_{\mathbf{k}} X^{0\sigma}_{\mathbf{k}} \rangle = Q\, n(\tilde{\varepsilon}_{\mathbf{k}})$. The prefactor $\eta = 2ma^2 t = t\,(p^2/2m)^{-1}$ is a dimensionless ratio of the hopping parameter t to the kinetic energy of an electron with the momentum p. In particular, for $a = 3.8$ Å and $t = 0.4$ eV, we have $\eta = 3.79\, t\,[\text{eV}] = 1.52$.

In these approximations, the relaxation rate (16) is determined by the expression

$$\Gamma(\omega) = t\, \frac{\pi(e^{\beta\omega}-1)}{\omega\, K(\delta)}\, \frac{3t^2\, Q^2}{2N^2} \sum_{\mathbf{k},\mathbf{q}} \int_{-\infty}^{\infty} d\omega'\, \chi''_{\pm}(\mathbf{q},\omega') \times \tilde{g}_x^2(\mathbf{k},\mathbf{k}-\mathbf{q})\, \delta(\tilde{\varepsilon}_{\mathbf{k}} - \tilde{\varepsilon}_{\mathbf{k}-\mathbf{q}} + \omega' - \omega) \times N(\omega')\, n(\tilde{\varepsilon}_{\mathbf{k}})\, [1 - n(\tilde{\varepsilon}_{\mathbf{k}-\mathbf{q}})], \quad (25)$$

where, using Eq. (17), the dimensionless transport vertex $\tilde{g}_x(\mathbf{k},\mathbf{k}-\mathbf{q}) = (1/at^2)\, g_x(\mathbf{k},\mathbf{k}-\mathbf{q})$ is introduced.

The real part of the conductivity (7) may be written as

$$\text{Re}\,\sigma(\omega) = A\,\tilde{\sigma}(\omega) \equiv A \frac{N_{\rm eff}\, t\, \Gamma(\omega)}{[\omega + M'(\omega)]^2 + [\Gamma(\omega)]^2}, \quad (26)$$

where $A = \omega_{0\rm pl}^2/(4\pi t) = e^2/(m v_0 t)$.

The real part of the memory function $M'(\omega) = \omega\,\lambda(\omega)$ is calculated by the dispersion relation (10) using the relaxation rate (25). This enables us to calculate the effective optical mass (8), $\tilde{m}/m = 1 + \lambda(0)$.

In numerical calculations, we take $J = 0.3\,t$ and $t = 0.4$ eV as an energy unit (0.4 eV = 3226 cm^{-1} = 4640 K). The results for the relaxation rate and the optical conductivity as functions of frequency, temperature, and hole doping are in a good overall agreement with experiments. This will be detailed in the following.

B. Relaxation rate

At zero frequency, the relaxation rate is related to the dimensionless electrical resistivity $\tilde{\rho} = 1/\tilde{\sigma}(0)$ by $\Gamma(0)/t = N_{\rm eff}\tilde{\rho}$. The temperature dependence of $\tilde{\rho}$ for $\delta = 0.09$, 0.16, and 0.20 is shown in Fig. 2. For a doping near and larger than the optimal doping ($\delta = 0.16$), we obtain a nearly linear temperature dependence, as is also observed in experiments (see, e.g., Refs. 61 and 62).

The effective number of charge carriers $N_{\rm eff}$ given by Eq. (24) is shown in the inset of Fig. 2. It does not reveal a notable temperature dependence and can be approximated by the function $N_{\rm eff} \simeq 2\,\delta$. It is remarkable that $N_{\rm eff}$ increases more rapidly than the hole doping. This result is in agreement with the in-plane optical conductivity data on LSCO compounds (Refs. 12 and 13), which yield the effective number of charge carriers $N_{\rm eff}(\omega)$ involved in optical excitations up to the cutoff frequency ω [upper limit of the integral in Eq. (4)]. $N_{\rm eff}$ was found to be nearly proportional to 2δ for doping $\delta < 0.15$, e.g., at $\delta = 0.1$, $N_{\rm eff}(\omega = 1.5\,\text{eV}) = 0.19$ (Fig. 11 in Ref. 12), and $N_{\rm eff}(\omega = 2\,\text{eV}) = 0.26$ (Fig. 10 in Ref. 13).

The frequency dependence of the relaxation rate $\Gamma(\omega)$ (25) at different temperatures and doping is plotted in Fig. 3. We obtain an increase of $\Gamma(\omega)$ with increasing temperature, which qualitatively agrees with experiments. In the overdoped case, the relaxation rate decreases resulting from the suppression

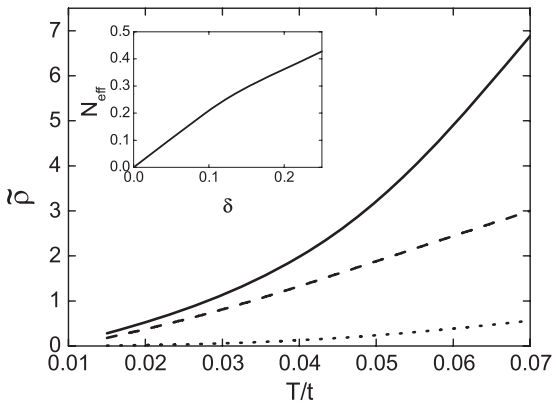

FIG. 2. Resistivity $\tilde{\rho}(T) = 1/\tilde{\sigma}(0,T)$ for doping $\delta = 0.09$ (solid line), 0.16 (dashed line), and 0.2 (dotted line). In the inset, the effective number of charge carriers $N_{\rm eff}(\delta)$ at $T = 0$ is shown.

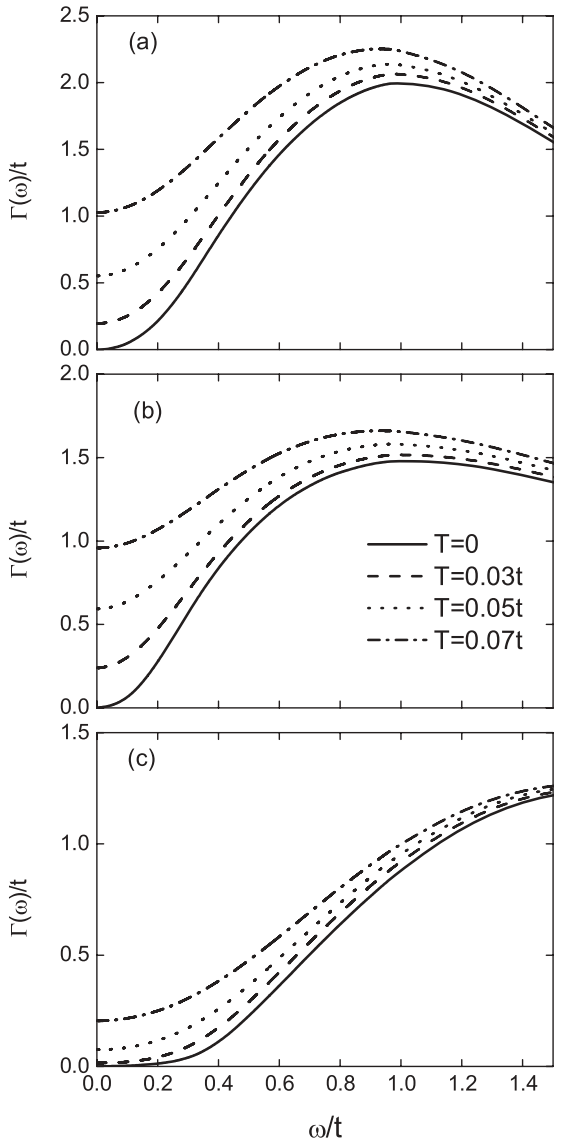

FIG. 3. Temperature dependence of the relaxation rate $\Gamma(\omega)$ for (a) $\delta = 0.09$, (b) 0.16, and (c) 0.2. Note the different scales.

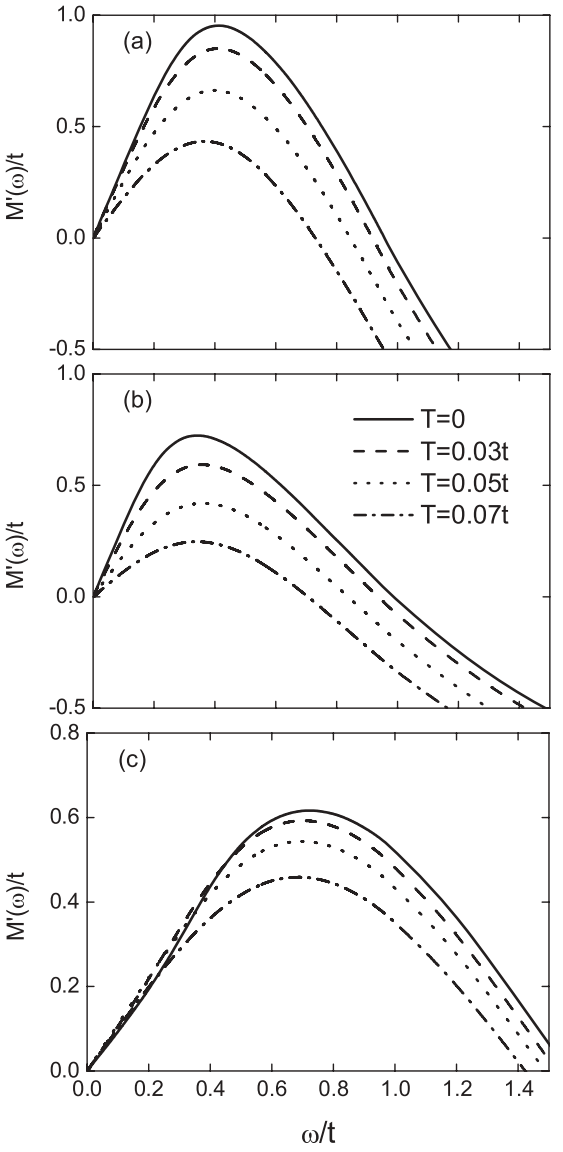

FIG. 4. Temperature dependence of the real part of the memory function $M'(\omega)$ for (a) $\delta = 0.09$, (b) 0.16, and (c) 0.2. Note the different scales.

of spin fluctuations. The broad maximum in the frequency dependence of $\Gamma(\omega)$, clearly revealed at low doping in Fig. 3(a), shifts to higher frequencies with increasing doping. The doping-dependent finite effective bandwidth $\widetilde{W}$ limits the highest frequency for the relaxation $\omega \leqslant 2\widetilde{W}$, so that at very high frequencies, $\Gamma(\omega)$ vanishes according to $\Gamma(\omega) \propto 1/\omega \to 0$. Let us point out that a maximum in the relaxation rate is also observed in experiments for the underdoped samples as, e.g., in $YBa_2Cu_3O_y$ ($YBCO_y$) at $\omega \sim 2000$ cm^{-1} for $y \lesssim 6.5$.[15]

The real part of the memory function $M'(\omega)$ shown in Fig. 4 exhibits a maximum height which decreases with increasing temperature and doping. But, the energy of the peak does not change with temperature as observed in experiments (see, e.g., Ref. 6–8). In the underdoped case ($\delta = 0.09$), the temperature dependence of $M'(\omega)$ is very strong, as compared with the overdoped case ($\delta = 0.2$). This results from the strong AF SRO at low doping that strongly depends on temperature. With increasing doping, both the SRO and the influence of temperature are weakened. Qualitatively, the relaxation rate (Fig. 3) reveals the same trend.

In Fig. 5, we show the temperature dependence of the effective optical mass at zero frequency $\widetilde{m}/m = 1 + \lambda(0)$ at various doping. At small doping, a strong temperature dependence of $\widetilde{m}/m$ is observed, which may be explained similarly as for $M'(\omega)$. For the overdoped case, the effective mass shows a weak renormalization $\widetilde{m}/m \sim 2$. In numerical studies of the one-hole motion in small clusters, a weak renormalization of the optical mass was deduced at high temperatures $T \gtrsim 0.2t$ (Ref. 35), which is in agreement with our results. In early experiments (Ref. 12), a large effective mass renormalization was obtained in LSCO ranging from $\widetilde{m}/m \simeq 25$ for $\delta = 0.1$ to $\widetilde{m}/m = 16$ for $\delta = 0.2$. However, later on, e.g., in Ref. 16, a nearly doping-independent modest renormalization of the effective mass $\widetilde{m}/m = 3{-}4$ was observed in both LSCO and YBCO, which is close to our finding.

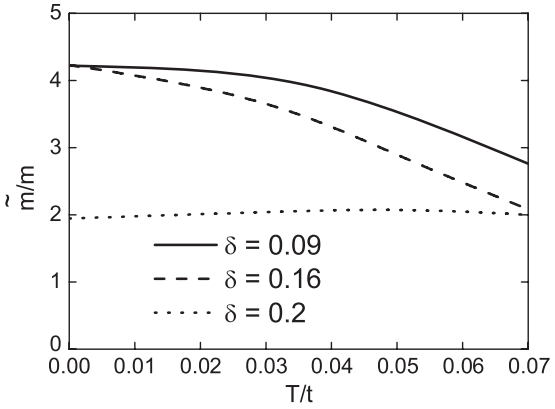

FIG. 5. Temperature dependence of the effective optical mass $\widetilde{m}/m = 1 + \lambda(0)$ at various doping.

C. Optical conductivity

The frequency dependence of the conductivity (26) for various temperatures and hole doping is shown in Fig. 6. The temperature and doping dependences of the conductivity show a reasonable qualitative agreement with experiments (see, e.g., Ref. 15). At low frequencies, a large Drude peak is found which significantly narrows at low temperatures. We also obtain a broad and nearly temperature-independent MIR maximum at $\omega \lesssim 2t \sim 6000\ \mathrm{cm}^{-1}$, which slightly shifts to lower frequencies and becomes of lower intensity with increasing doping as observed in experiments (see, e.g., Ref. 16). In our theory, the MIR absorption results from electron interaction with spin fluctuations which influence the electron scattering so that it decreases with increasing doping.

D. Quantitative comparison to experiments

Let us first compare the resistivity $\rho(T) = (1/A)\,\widetilde{\rho}$, where A is given in Eq. (26), with experimental data for the underdoped cuprate $YBCO_{6.5}$ ($\delta = 0.09$) (Ref. 6) shown in Fig. 7(a). Here, we use the value $A = e^2/(m v_0 t) = 8.00 \times 10^3 [\Omega\ \mathrm{cm}]^{-1}$ taking $v_0 = 57.7\ (\text{Å})^3$.[6] Without a fitting procedure, we obtain a remarkably good agreement with experiment, both in the absolute values of the resistivity and in its temperature dependence. In Fig. 7(b), we compare the resistivity $\rho(T)$ with experimental data on LSCO (Ref. 61) for the underdoped ($\delta = 0.08$) and nearly optimally doped ($\delta = 0.17$) samples with our results. The value of $A = 4.86 \times 10^3\ [\Omega\,\mathrm{cm}]^{-1}$ is obtained using $v_0 = a^2 d = 95.3\ (\text{Å})^3$ ($a = 3.8$ Å and $d = 6.6$ Å). A reasonable agreement is observed at high temperatures, while at low temperatures our values are much smaller. An additional scattering mechanism, e.g., impurity scattering, should be invoked to explain the experimental data. The comparison of our results with optimally doped and overdoped Tl compounds[63] shows the same trend.

Now, we estimate the plasma frequency $\omega_{\mathrm{pl}} = [N_{\mathrm{eff}}]^{1/2}\omega_{0,\mathrm{pl}}$. For the optimally doped case $\delta = 0.16$, we have $N_{\mathrm{eff}} = 0.3$ and $\omega_{\mathrm{pl}} = 0.55\,\omega_{0,\mathrm{pl}}$. For LSCO ($\omega_{0,\mathrm{pl}} = 3.72$ eV), we get $\omega_{\mathrm{pl}} = 2.05$ eV and for YBCO ($\omega_{0,\mathrm{pl}} = 3.96$ eV), $\omega_{\mathrm{pl}} = 2.18$ eV. These values are close to experiments, while the LDA calculations in Ref. 64 give the somewhat larger value $\omega_{\mathrm{pl}} \approx 2.9$ eV. For the underdoped $YBCO_{6.5}$ crystal, $\omega_{\mathrm{pl}} = 1.89$ eV,[6] while for $\delta = 0.09$ we have $N_{\mathrm{eff}} = 0.18$ and $\omega_{\mathrm{pl}} = 1.68$ eV, which is close to the experimental value.

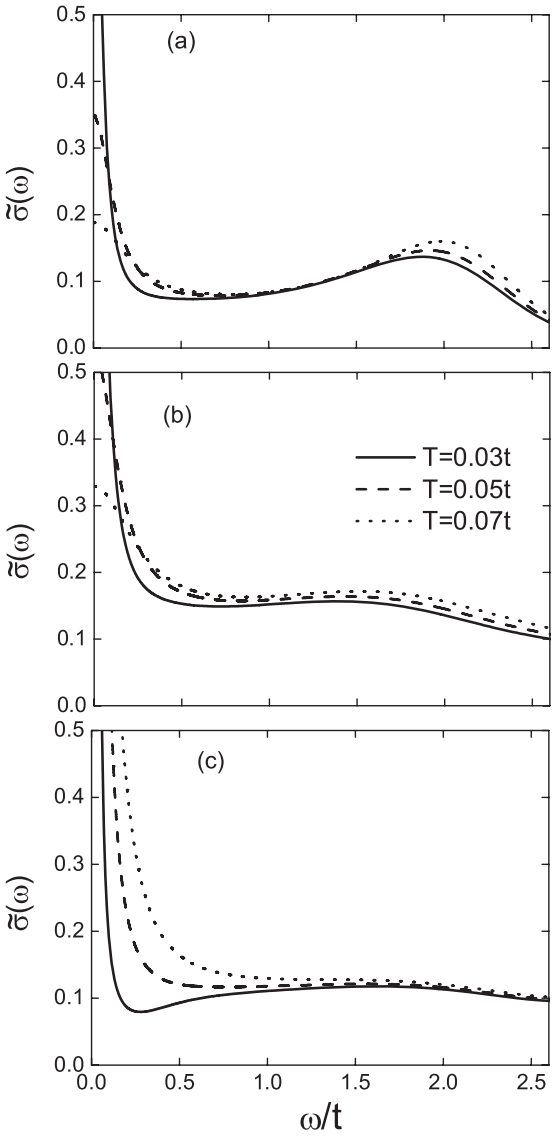

FIG. 6. Temperature dependence of the optical conductivity $\widetilde{\sigma}(\omega)$ for (a) $\delta = 0.09$, (b) 0.16, and (c) 0.2.

Finally, let us compare the relaxation rate $\Gamma(\omega)$ with the optical data for $YBCO_{6.5}$ given in Ref. 6. In the frequency region $\omega \leqslant 1500\ \mathrm{cm}^{-1}$ and for the temperatures $T = 0.03t$ and $0.05t$, which are close to the experimental values $T = 147$ and 244 K, respectively, we get the results shown in Fig. 8. As we see, for the optical properties, we also obtain a reasonable quantitative agreement of our theory with experiments.

E. Comparison with previous theoretical studies

Various methods have been used in theoretical studies of the optical and dc conductivities in cuprates as discussed in Sec. I. Here, we compare our results with previous studies to clarify what kind of problems the latter has and how we have resolved some of them.

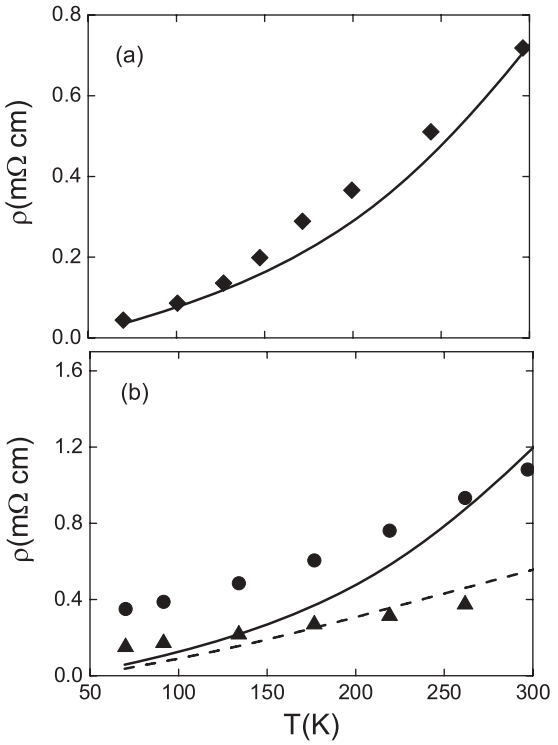

FIG. 7. Temperature dependence of the resistivity $\rho(T)$ at (a) $\delta = 0.09$ in comparison with the experimental data for $YBCO_{6.5}$ from Ref. 6 shown by symbols, and (b) at $\delta = 0.08$ (solid line) and $\delta = 0.17$ (dashed line) in comparison with the experimental data for LSCO from Ref. 61 shown by symbols.

One of the problems is how to explain a linear temperature dependence of the resistivity in optimally doped cuprates in a broad temperature range (see, e.g., Ref. 65 and a discussion in Ref. 62). In early studies, the local density functional theory was used in the calculation of transport properties of cuprates (for a review, see Ref. 64). Calculations of the resistivity within the relaxation rate approximation for electron scattering on phonons, $(1/\tau_{tr}) \propto \lambda_{tr} T$, result in a linear T dependence over a broad temperature range $\rho \propto 1/(\tau_{tr}\omega_{pl}^2)$. However, the absolute values of the resistivity prove to be several times smaller than the experimental ones. This discrepancy could

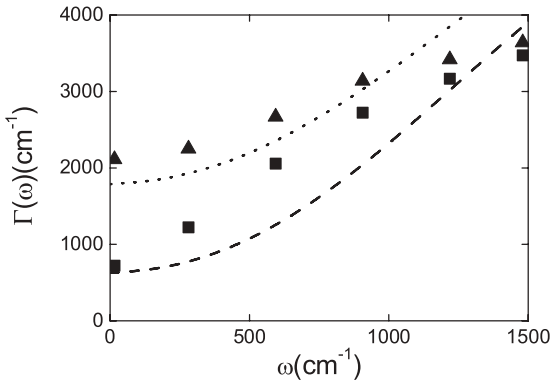

FIG. 8. Relaxation rate $\Gamma(\omega)$ at $\delta = 0.09$ for $T = 0.03t$ (dashed line) and $T = 0.05t$ (dotted line) in comparison with experimental data for $YBCO_{6.5}$ (Ref. 6) shown by symbols: squares for $T = 147$ K and triangles for $T = 244$ K.

be removed by using larger values of the transport EPI coupling constant $\lambda_{tr} = 1.5$–2 instead of the calculated value $\lambda_{tr} = 0.65$–0.32 for optimally doped LSCO and YBCO, or by assuming the theoretical plasma frequencies ω_{pl} to be smaller by a factor of 2 to 3.

To reconcile a weak transport EPI coupling $\lambda_{tr} \sim 0.5$ and a strong EPI for quasiparticles $\lambda_{qp} \sim 2$, needed to explain the high T_c in cuprates, a model of a strong forward scattering of electrons induced by electron correlations was proposed[66] which enables the authors to obtain $\lambda_{tr} \sim \lambda_{qp}/3$ (for a review, see Ref. 11, Sec. III B). This model was used in Ref. 67 to explain a linear T dependence of the resistivity in a broad region of T where, however, the extended van Hove singularities sufficiently close to the Fermi energy were assumed and fitting parameters for EPI were introduced.

As shown in Fig. 7(b), we obtain a linear temperature dependence for the resistivity for a nearly optimally doped sample in a reasonable agreement with experiment on LSCO without using fitting parameters. The values of the plasma frequency are also close to experiments. In our memory-function theory, the transport relaxation rate $\Gamma(\omega)$ and the quasiparticle self-energy are not related in a simple way, and therefore we can explain a sufficiently weak scattering observed in the conductivity and a strong superconducting pairing induced by the same electron coupling to spin fluctuations (see, e.g., Ref. 68).

To describe the normal-state properties, such as the resistivity and OC, phenomenological spin-fermion models have been used. In particular, within a nearly antiferromagnetic Fermi-liquid model,[69] a reasonable agreement with experiments on resistivity for $YBCO_7$ (Ref. 70) and on OC for optimally doped and overdoped cuprate compounds[71] was obtained by a particular choice of model parameters. In Ref. 72, the OC of $YBCO_x$ ($x = 6.3, 7$) within the memory-function method was calculated. To obtain an agreement with experiments, several models for the spin susceptibility have to be considered. A detailed qualitative discussion of the OC behavior at various frequencies and temperatures within the spin-fermion model was performed in Ref. 42. Contrary to these phenomenological approaches, we obtain a fair agreement with experiments for various doping and temperatures within the microscopic theory for the spin-fluctuation susceptibility without fitting coupling parameters.

There are several studies of the OC within the Hubbard model in the limit of weak correlations, where the insulating AF state emerges from a strong AF interaction as discussed in Sec. I. In particular, in Ref. 73, the OC was calculated based on a self-consistent treatment of the Hubbard model. It was argued that the charge-transfer gap observed in the insulating state of cuprates is due to the AF LRO which splits the CuO_2 band into two magnetic subbands. Assuming that the AF LRO exists at any doping, the experimentally observed increase of the charge-transfer energy with doping and a simultaneous decrease of the MIR absorption energy were explained. In this scenario, the MIR band originates from the pseudogap in the electronic spectrum also induced by the AF LRO. In our theory, based on the consideration of the $t - J$ model, we can not study the interesting problem of doping dependence of the charge-transfer peak at high energy observed in the insulator-to-metal transition in cuprates. This problem should

be considered within the two-subband Hubbard model as, e.g., in Ref. 74, since in the $t-J$ model only the lower Hubbard subband is explicitly taken into account.

In Ref. 39, the MIR absorption in the region of $\omega \approx t-2t$, being quite strong even without coupling to phonons, was related to the interaction of a doped hole with spin excitations. In our theory, we can explain the MIR absorption by electron interaction with spin fluctuations in the decay of charge excitations. We can not relate the MIR absorption to the pseudogap in the single-particle electronic spectrum since the MIR conductivity shows no notable temperature and doping dependence, which is characteristic for the pseudogap phenomenon.[75]

In the limit of strong correlations, the Hubbard model and $t-J$ model have been used in calculations of dc and optical conductivity. As was pointed out in Sec. I, in numerical studies of finite clusters, due to a finite energy resolution, only restricted information on the frequency and temperature dependence of the OC can be found. The effects of strong correlations have been efficiently taken into account within the DMFT method, which enables the authors to reproduce qualitatively the main features of the OC: the Drude peak, the MIR region, the charge-transfer excitations, and the temperature and doping dependence of the optical spectral weight (see, e.g., Refs. 21, 76, and 77 and references therein). However, in the DMFT, the spatial correlations, such as short-range AF fluctuations, are not taken into account, and therefore the low-energy part of the OC caused by charge-boson interaction can not be studied. In the cluster DMFT,[28] due to a finite size of clusters, only a qualitative low-frequency behavior of the OC can be found. In this work, the complicated wave-vector dependence of the dynamical spin susceptibility and the electron interaction with spin fluctuations are fully taken into account without using fitting parameters. This enables us to reproduce both the transport relaxation rate $\Gamma(\omega,T)$ (see Fig. 3) and the real part of the memory function $M'(\omega,T)$ (see Fig. 4), yielding the optical mass renormalization, in a fair agreement with experiments.

The Allen approximation[40] for the current-current correlation function, commonly used in the calculation of the OC and the transport relaxation rate $1/\tau$, is based on the perturbation theory with respect to $(1/\omega\tau) \ll 1$. In our memory-function approach, the optical relaxation rate (16) describes the direct decay of a charge excitation into an electron-hole pair assisted by the excitation of spin fluctuations. In the Allen approach, processes of this type appear due to finite lifetime effects for the electron-hole pair. Therefore, to calculate the optical relaxation rate, one has to express the latter in terms of a quasiparticle scattering rate, which is not a straightforward procedure (see, e.g., Refs. 78–80).

The present microscopic theory has in fact some limitations arising from the $t-J$ model used in the calculations. Besides the deficiency of the charge-transfer peak at high energy discussed above, the complicated structure of the OC found experimentally in the MIR region is missed in our theory. This may be due to polaron effects and the coupling of magnetic excitations with phonons via doped holes as discussed in Refs. 37–39. To overcome these limitations, an extended Hubbard model, including a strong electron-phonon interaction, should be considered.

V. CONCLUSION

In this paper, we have studied the charge dynamics within a microscopic theory for the optical and dc conductivities for the $t-J$ model by taking into account electron scattering by spin fluctuations. In our theory, based on the memory-function formalism, we calculate directly the transport relaxation rate without using the Allen perturbation theory.

Within the proposed theory, we are able to obtain a reasonable agreement with experiments on cuprates for the relaxation rate, the optical conductivity, and the resistivity in broad regions of temperatures and doping. In particular, in the underdoped region with a strong AF SRO, a fair quantitative agreement was found for the resistivity [Fig. 7(a)] and for the relaxation rate (Fig. 8). This proves the essential role of AF spin fluctuations in the charge dynamics of cuprates. This conclusion has been corroborated in a number of theoretical and experimental studies of OC (see, e.g., Refs. 7 and 8 and references therein). In the overdoped case, where the AF spin fluctuations are suppressed, additional scattering mechanisms (e.g., due to electron-phonon interaction and impurity scattering) should be invoked to explain experimental data. From our results, we conclude that spin fluctuations induced by the kinematic interaction should give a substantial contribution to the d-wave pairing in cuprates as has been shown recently in Ref. 68.

ACKNOWLEDGMENTS

Partial financial support by the Heisenberg-Landau Program of JINR is acknowledged. One of the authors (N.P.) is grateful to the MPIPKS, Dresden, for the hospitality during his stay at the Institute, where a part of this work has been done.

APPENDIX A: CALCULATION OF THE MEMORY FUNCTION

To derive Eq. (6) for the memory function, we consider the equations of motion for the relaxation function $\Phi(t-t') = \langle\langle J_x(t)|J_x(t')\rangle\rangle$ (see Refs. 45, 47, and 74). Differentiating the function subsequently over time t and t', we obtain a system of equations which in the Fourier representation read as

$$\omega\,\Phi(\omega) = \chi_0 + \langle\langle F_x|J_x\rangle\rangle_\omega, \tag{A1}$$

$$\omega\,\langle\langle F_x|J_x\rangle\rangle_\omega = -\langle\langle F_x|F_x\rangle\rangle_\omega, \tag{A2}$$

where $F_x = i\dot{J}_x = [J_x,H]$ is the force operator. In Eq. (A2), the relation of the orthogonality $(F_x,J_x) = (i\dot{J}_x,J_x) = \langle[J_x,J_x]\rangle = 0$ was used. Introducing the zero-order relaxation function $\Phi_0(\omega) = \chi_0/\omega$, we can solve the system of equations (A1) and (A2) in the form

$$\Phi(\omega) = \Phi_0(\omega) - \Phi_0(\omega)\,T(\omega)\,\Phi_0(\omega), \tag{A3}$$

with the scattering matrix

$$T(\omega) = (1/\chi_0)\langle\langle F_x|F_x\rangle\rangle_\omega(1/\chi_0). \tag{A4}$$

The memory function $M(\omega)$ is defined by Eq. (5), which can be written in the form

$$\Phi(\omega) = \Phi_0(\omega) - \Phi_0(\omega)\,[M(\omega)/\chi_0]\,\Phi(\omega). \tag{A5}$$

From Eqs. (A3) and (A5), we get a relation between the memory function and the scattering matrix:

$$T(\omega) = [M(\omega)/\chi_0] - [M(\omega)/\chi_0]\Phi_0(\omega)T(\omega). \quad \text{(A6)}$$

This equation shows that the memory function is the "proper part" of the scattering matrix (A4) which has no parts connected by a single zero-order relaxation function, i.e., $M(\omega) = \chi_0 T(\omega)^{\text{proper}}$ as given by Eq. (6).

APPENDIX B: MODE-COUPLING APPROXIMATION

Using the spectral representation for the retarded Green's functions,[56] we write the relaxation rate (9), $\Gamma(\omega) = M''(\omega) = \text{Im}\langle\langle F_x|F_x\rangle\rangle^{\text{proper}}_{\omega+i0^+}(1/\chi_0)$, in terms of the time-dependent force-force correlation function

$$\Gamma(\omega) = \pi\frac{1-\exp(\beta\omega)}{2\chi_0\omega}\int_{-\infty}^{\infty} dt\, e^{i\omega t}\langle F_x F_x(t)\rangle^{\text{proper}}. \quad \text{(B1)}$$

To calculate the force operator $F_x = [J_x, H]$, we first determine the current $J_x = -i[P_x, H]$, where the polarization operator in terms of HOs reads as $P_x = e\sum_i R_i^x \sum_\sigma X_i^{\sigma\sigma}$. Using the commutation relations (13), we derive the expression for the current operator

$$J_x = ie\sum_{i,j,\sigma}\left(R_i^x - R_j^x\right) t_{ij}\; X_i^{\sigma 0} X_j^{0\sigma}. \quad \text{(B2)}$$

The force operator describes electron scattering on spin and charge (density) excitations which results from the kinematic interaction for the HOs. This can be seen from the equation of motion for the electron annihilation operator

$$i\frac{d}{dt}X_i^{0\sigma}(t) = \left[X_i^{0\sigma}, H\right] = -\mu X_i^{0\sigma} - \sum_{j,\sigma'} t_{ij} B_{i\sigma\sigma'} X_j^{0\sigma'} + (1/2)\sum_{j,\sigma'} J_{ij}\; X_i^{0\sigma'}[B_{j\sigma\sigma'} - \delta_{\sigma'\sigma}], \quad \text{(B3)}$$

where the Bose-type operator $B_{i\sigma\sigma'}$ is introduced:

$$B_{i\sigma\sigma'} = \left(X_i^{00} + X_i^{\sigma\sigma}\right)\delta_{\sigma'\sigma} + X_i^{\bar{\sigma}\sigma}\delta_{\sigma'\bar{\sigma}} = \left[1 - (1/2)N_j + S_j^z\right]\delta_{\sigma'\sigma} + S_j^{\bar{\sigma}}\delta_{\sigma'\bar{\sigma}}. \quad \text{(B4)}$$

Here, the completeness relation for the HOs and the definition of the number and spin operators (14) are used. By this type of equations of motion, for the force operator we obtain the expression

$$F_x = -ie\sum_{i,j,l}\sum_{\sigma\sigma'}\left(R_i^x - R_j^x\right) t_{ij} \times \left\{X_i^{\sigma 0}\left[t_{jl}X_l^{0\sigma'}B_{j\sigma\sigma'} - (1/2)J_{jl}\; X_j^{0\sigma'}B_{l\sigma\sigma'}\right] - \left[t_{il}X_l^{\sigma' 0}B^\dagger_{i\sigma\sigma'} - (1/2)J_{il}\; X_i^{\sigma' 0}B^\dagger_{l\sigma\sigma'}\right]X_j^{0\sigma}\right\}. \quad \text{(B5)}$$

Introducing the $\mathbf{q}$ representation for HOs and the interactions

$$X_i^{0\sigma} = \frac{1}{\sqrt{N}}\sum_{\mathbf{q}} X_{\mathbf{q}}^{0\sigma}\; e^{i\mathbf{q}\mathbf{R}_i}, \quad B_{j\sigma\sigma'} = \frac{1}{N}\sum_{\mathbf{q}} B_{\mathbf{q}\sigma\sigma'}\; e^{i\mathbf{q}\mathbf{R}_j},$$
$$t_{ij} = \frac{1}{N}\sum_{\mathbf{q}} t(\mathbf{q})\, e^{i\mathbf{q}\mathbf{R}_{ij}}, \quad J_{ij} = \frac{1}{N}\sum_{\mathbf{q}} J(\mathbf{q})\, e^{i\mathbf{q}\mathbf{R}_{ij}}, \quad \text{(B6)}$$

where $\mathbf{R}_{ij} = \mathbf{R}_i - \mathbf{R}_j$, the force operator (B5) takes the form

$$F_x = -\frac{e}{N}\sum_{\mathbf{k},\mathbf{q}}\sum_{\sigma\sigma'} v_x(\mathbf{k})\,[t(\mathbf{k}-\mathbf{q}) - (1/2)J(\mathbf{q})] \times \left\{X_{\mathbf{k}}^{\sigma 0}X_{\mathbf{k}-\mathbf{q}}^{0\sigma'}\,B_{\mathbf{q}\sigma\sigma'} - X_{\mathbf{k}-\mathbf{q}}^{\sigma' 0}X_{\mathbf{k}}^{0\sigma}\;B_{-\mathbf{q}\sigma'\sigma}\right\}, \quad \text{(B7)}$$

where $v_x(\mathbf{k}) = -\partial t(\mathbf{k})/\partial k_x$ is the electron velocity. Changing the indexes in the last term, $\mathbf{k}' = \mathbf{k} - \mathbf{q}$, $\sigma \leftrightarrow \sigma'$, and $\mathbf{q} \to -\mathbf{q}$, we obtain the final expression

$$F_x = -\frac{e}{N}\sum_{\mathbf{k},\mathbf{q}}\sum_{\sigma\sigma'}\{\, v_x(\mathbf{k})\,[t(\mathbf{k}-\mathbf{q}) - (1/2)J(\mathbf{q})] - v_x(\mathbf{k}-\mathbf{q})\,[t(\mathbf{k}) - (1/2)J(\mathbf{q})]\}X_{\mathbf{k}}^{\sigma 0}X_{\mathbf{k}-\mathbf{q}}^{0\sigma'}B_{\mathbf{q}\sigma\sigma'}$$
$$\equiv -\frac{e}{N}\sum_{\mathbf{k},\mathbf{q}}\sum_{\sigma\sigma'} g_x(\mathbf{k},\mathbf{k}-\mathbf{q})\, X_{\mathbf{k}}^{\sigma 0}X_{\mathbf{k}-\mathbf{q}}^{0\sigma'}\,B_{\mathbf{q}\sigma\sigma'}. \quad \text{(B8)}$$

In the last equation, we introduce the transport vertex $g_x(\mathbf{k},\mathbf{k}-\mathbf{q})$ given by Eq. (17).

We calculate the many-particle time-dependent correlation functions in Eq. (B1) in the mode-coupling approximation assuming an independent propagation of electron and charge-spin excitations. In this approximation, the time-dependent correlation functions can be written as a product of fermionic and bosonic correlation functions:

$$\left\langle X_{\mathbf{k}}^{\sigma 0}X_{\mathbf{k}-\mathbf{q}}^{0\sigma'}B_{\mathbf{q}\sigma\sigma'}\middle|X_{\mathbf{k}-\mathbf{q}}^{\sigma' 0}(t)X_{\mathbf{k}}^{0\sigma}(t)B^\dagger_{\mathbf{q}\sigma\sigma'}(t)\right\rangle = \left\langle X_{\mathbf{k}}^{\sigma 0}X_{\mathbf{k}}^{0\sigma}(t)\right\rangle\left\langle X_{\mathbf{k}-\mathbf{q}}^{0\sigma'}X_{\mathbf{k}-\mathbf{q}}^{\sigma' 0}(t)\right\rangle\langle B_{\mathbf{q}\sigma\sigma'}B^\dagger_{\mathbf{q}\sigma\sigma'}(t)\rangle\ . \quad \text{(B9)}$$

Using the definition for the Bose-type operator (B4), for the bosonic correlation function we obtain

$$\begin{aligned}
&\langle B_{\mathbf{q}\sigma\sigma'}B^\dagger_{\mathbf{q}\sigma\sigma'}(t)\rangle \\
&= \left\langle\left\{\left[X_{\mathbf{q}}^{00} + X_{\mathbf{q}}^{\sigma\sigma}\right]\delta_{\sigma'\sigma} + X_{\mathbf{q}}^{\bar{\sigma}\sigma}\,\delta_{\sigma'\bar{\sigma}}\right\}\right. \\
&\quad\left.\times\left\{\left[X_{-\mathbf{q}}^{00}(t) + X_{-\mathbf{q}}^{\sigma\sigma}(t)\right]\delta_{\sigma'\sigma} + X_{-\mathbf{q}}^{\sigma\bar{\sigma}}(t)\,\delta_{\sigma'\bar{\sigma}}\right\}\right\rangle \\
&= \left\langle\left\{X_{\mathbf{q}}^{00} + X_{\mathbf{q}}^{\sigma\sigma}\right\}\left\{X_{-\mathbf{q}}^{00}(t) + X_{-\mathbf{q}}^{\sigma\sigma}(t)\right\}\right\rangle\delta_{\sigma'\sigma} \\
&\quad + \left\langle X_{\mathbf{q}}^{\bar{\sigma}\sigma}X_{-\mathbf{q}}^{\sigma\bar{\sigma}}(t)\right\rangle\delta_{\sigma'\bar{\sigma}} \\
&= (1/4)\langle N_{\mathbf{q}}N_{-\mathbf{q}}(t)\rangle\,\delta_{\sigma'\sigma} \\
&\quad + \left\langle S_{\mathbf{q}}^z S_{-\mathbf{q}}^z(t)\right\rangle\delta_{\sigma'\sigma} + \left\langle X_{\mathbf{q}}^{\bar{\sigma}\sigma}X_{-\mathbf{q}}^{\sigma\bar{\sigma}}(t)\right\rangle\delta_{\sigma'\bar{\sigma}}. \qquad \text{(B10)}
\end{aligned}$$

In the paramagnetic state, for the sum of the spin correlation functions in Eq. (B10), we have $\langle S_{\mathbf{q}}^z S_{-\mathbf{q}}^z(t)\rangle + \langle S_{\mathbf{q}}^- S_{-\mathbf{q}}^+(t)\rangle = \langle \mathbf{S}_{\mathbf{q}}\mathbf{S}_{-\mathbf{q}}(t)\rangle$. Finally, using spectral representations for the time-dependent correlation functions in Eq. (B9),[56]

$$\langle BA(t)\rangle = \int_{-\infty}^{\infty} d\omega\, e^{-i\omega t} f(\omega)[-(1/\pi)]\text{Im}\langle\langle A|B\rangle\rangle_\omega, \quad \text{(B11)}$$

where $f(\omega)$ is the Fermi function $n(\omega)$ for the correlation function $\langle X_{\mathbf{k}}^{\sigma 0}X_{\mathbf{k}}^{0\sigma}(t)\rangle$ and the Bose function $N(\omega)$ for the charge-spin correlation functions, after integration over time t in Eq. (B1) we obtain the expression (16) for the relaxation rate.

[1] T. Timusk and D. Tanner, in *Physical Properties of High Temperature Superconductors III*, edited by D. M. Ginsberg (World Scientific, Singapore, 1992), Chap. 5.

[2] D. N. Basov and T. Timusk, Rev. Mod. Phys. **77**, 721 (2005).

[3] D. N. Basov, R. D. Averitt, D. van der Marel, M. Dressel, and K. Haule, Rev. Mod. Phys. **83**, 471 (2011).

[4] N. M. Plakida, *High-Temperature Cuprate Superconductors*. (Springer, Heidelberg, 2010), Chap. 5.

[5] A. A. Kordyuk, V. B. Zabolotnyy, D. V. Evtushinsky, D. S. Inosov, T. K. Kim, B. Büchner, and S. V. Borisenko, Eur. Phys. J. Special Topics **188**, 153 (2010).

[6] J. Hwang, J. Yang, T. Timusk, S. G. Sharapov, J. P. Carbotte, D. A. Bonn, R. Liang, and W. N. Hardy, Phys. Rev. B **73**, 014508 (2006).

[7] J. Yang, J. Hwang, E. Schachinger, J. P. Carbotte, R. P. S. M. Lobo, D. Colson, A. Forget, and T. Timusk, Phys. Rev. Lett. **102**, 027003 (2009).

[8] E. van Heumen, E. Muhlethaler, A. B. Kuzmenko, H. Eisaki, W. Meevasana, M. Greven, and D. van der Marel, Phys. Rev. B **79**, 184512 (2009).

[9] Ph. Bourges, in *The Gap Symmetry and Fluctuations in High Temperature Superconductors*, edited by J. Bok, G. Deutscher, D. Pavuna, and S. A. Wolf (Plenum, New York, 1998), pp. 349–371.

[10] M. Le Tacon *et al*., Nat. Phys. **7**, 725 (2011).

[11] E. G. Maksimov, M. L. Kulić, and O. V. Dolgov, Adv. Cond. Mat. Physics **2010**, 423725 (2010).

[12] S. Uchida, T. Ido, H. Takagi, T. Arima, Y. Tokura, and S. Tajima, Phys. Rev. B **43**, 7942 (1991).

[13] S. Uchida, K. Tamasaku, and S. Tajima, Phys. Rev. B **53**, 14558 (1996).

[14] Y. Onose, Y. Taguchi, K. Ishizaka, and Y. Tokura, Phys. Rev. B **69**, 024504 (2004).

[15] Y. S. Lee, K. Segawa, Z. Q. Li, W. J. Padilla, M. Dumm, S. V. Dordevic, C. C. Homes, Y. Ando, and D. N. Basov, Phys. Rev. B **72**, 054529 (2005).

[16] W. J. Padilla, Y. S. Lee, M. Dumm, G. Blumberg, S. Ono, K. Segawa, S. Komiya, Y. Ando, and D. N. Basov, Phys. Rev. B **72**, 060511(R) (2005).

[17] S. Lupi, D. Nicoletti, O. Limaj, L. Baldassarre, M. Ortolani, S. Ono, Yoichi Ando, and P. Calvani, Phys. Rev. Lett. **102**, 206409 (2009).

[18] Y. Iye, in *Properties of High Temperature Superconductors*, edited by D. M. Ginsberg, Vol. 3 (World Scientific, Singapore, 1992), pp. 285–361.

[19] J. Zaanen, G. A. Sawatzky, and J. W. Allen, Phys. Rev. Lett. **55**, 418 (1985).

[20] P. A. Lee, N. Nagaosa, and X.-G. Wen, Rev. Mod. Phys. **78**, 17 (2006).

[21] A. Comanac, L. De' Medici, M. Capone, and A. J. Millis, Nat. Phys. **4**, 287 (2008).

[22] A. Georges, B. G. Kotliar, W. Krauth, and M. J. Rozenberg, Rev. Mod. Phys. **68**, 13 (1996).

[23] C. Weber, K. Haule, and G. Kotliar, Phys. Rev. B **78**, 134519 (2008).

[24] C. Weber, K. Haule, and G. Kotliar, Nat. Phys. **6**, 574 (2010).

[25] G. Kotliar, S. Y. Savrasov, K. Haule, V. S. Oudovenko, O. Parcollet, and C. A. Marianetti, Rev. Mod. Phys. **78**, 865 (2006).

[26] N. M. Plakida and V. S. Oudovenko, Zh. Exp. Theor. Phys. **131**, 259 (2007) [JETP **104**, 230 (2007)].

[27] K. Haule and G. Kotliar, Phys. Rev. B **76**, 104509 (2007).

[28] K. Haule and G. Kotliar, Europhys. Lett. **77**, 27007 (2007).

[29] F. Carbone, A. B. Kuzmenko, H. J. A. Molegraaf, E. van Heumen, V. Lukovac, F. Marsiglio, D. van der Marel, K. Haule, G. Kotliar, H. Berger, S. Courjault, P. H. Kes, and M. Li, Phys. Rev. B **74**, 064510 (2006).

[30] N. Bontemps, R. P. S. M. Lobo, A. F. Santander-Syro, and A. Zimmers, Ann. Phys. (NY) **321**, 1547 (2006).

[31] E. Dagotto, Rev. Mod. Phys. **66**, 763 (1994).

[32] W. Stephan and P. Horsch, Int. J. Mod. Phys. B **6**, 589 (1992).

[33] T. Tohyama, P. Horsch, and S. Maekawa, Phys. Rev. Lett. **74**, 980 (1995).

[34] R. Eder, Y. Ohta, and S. Maekawa, Phys. Rev. Lett. **74**, 5124 (1995).

[35] J. Jaklič and P. Prelovšek, Adv. Phys. **49**, 1 (2000).

[36] M. Vojta and K. W. Becker, Eur. Phys. J. B **3**, 427 (1998).

[37] E. Cappelluti, S. Ciuchi, and S. Fratini, Phys. Rev. B **76**, 125111 (2007).

[38] A. S. Mishchenko, N. Nagaosa, Z.-X. Shen, G. De Filippis, V. Cataudella, T. P. Devereaux, C. Bernhard, K. W. Kim, and J. Zaanen, Phys. Rev. Lett. **100**, 166401 (2008).

[39] L. Vidmar, J. Bonča, and S. Maekawa, Phys. Rev. B **79**, 125120 (2009).

[40] P. B. Allen, Phys. Rev. B **3**, 305 (1971).

[41] S. V. Shulga, O. V. Dolgov, and E. G. Maksimov, Phys. C (Amsterdam) **178**, 266 (1991).

[42] Ar. Abanov, A. V. Chubukov, and J. Schmalian, Adv. Phys. **52**, 119 (2003).

[43] A. V. Chubukov, D. Pines, and J. Schmalian, in *The Physics of Conventional and Unconvencional Superconductors*, edited by K. H. Bennemann and J. B. Ketterson, Vol. 1 (Springer, Heidelberg, 2004), p. 495.

[44] H. Mori, Prog. Theor. Phys. **34**, 399 (1965).

[45] W. Götze and P. Wölfle, J. Low Temp. Phys. **5**, 575 (1971); Phys. Rev. B **6**, 1226 (1972).

[46] D. Ihle and N. M. Plakida, Z. Phys. B **96**, 159 (1994).

[47] N. M. Plakida, Z. Phys. B **103**, 383 (1997).

[48] A. A. Vladimirov, D. Ihle, and N. M. Plakida, Phys. Rev. B **80**, 104425 (2009).

[49] A. A. Vladimirov, D. Ihle, and N. M. Plakida, Phys. Rev. B **83**, 024411 (2011).

[50] R. Kubo, J. Phys. Soc. Jpn. **12**, 570 (1957).

[51] P. W. Anderson, Science **235**, 1196 (1987).

[52] F. C. Zhang and T. M. Rice, Phys. Rev. B **37**, 3759 (1988).

[53] J. Hubbard, Proc. R. Soc. A **285**, 542 (1965).

[54] Yu. A. Izyumov and Yu. N. Scryabin, *Statistical Mechanics of Magnetically Ordered Systems* (Consultant Bureau, New York, 1989), pp. 74–108.

[55] F. Dyson, Phys. Rev. **102**, 1217 (1956).

[56] D. N. Zubarev, Sov. Phys.–Usp. **3**, 320 (1960).

[57] G. Jackeli and N. M. Plakida, Phys. Rev. B **60**, 5266 (1999).

[58] N. M. Plakida and V. S. Oudovenko, Phys. Rev. B **59**, 11949 (1999).

[59] A. A. Kordyuk, S. V. Borisenko, A. Koitzsch, J. Fink, M. Knupfer, and H. Berger, Phys. Rev. B **71**, 214513 (2005).

[60] P. Prelovšek and A. Ramšak, Phys. Rev. B **65**, 174529 (2002).

[61] G. S. Boebinger, Y. Ando, A. Passner, T. Kimura, M. Okuya, J. Shimoyama, K. Kishio, K. Tamasaku, N. Ichikawa, and S. Uchida, Phys. Rev. Lett. **77**, 5417 (1996).

[62] Y. Ando, S. Komiya, K. Segawa, S. Ono, and Y. Kurita, Phys. Rev. Lett. **93**, 267001 (2004).

[63] Y. C. Ma and N. L. Wang, Phys. Rev. B **73**, 144503 (2006).

[64] W. E. Pickett, Rev. Mod. Phys. **61**, 433 (1989).

[65]T. A. Friedmann, M. W. Rabin, J. Giapintzakis, J. P. Rice, and D. M. Ginsberg, Phys. Rev. B **42**, 6217 (1990).
[66]R. Zeyher and M. L. Kulić, Phys. Rev. B **53**, 2850 (1996).
[67]G. Varelogiannis and E. N. Economou, Europhys. Lett. **42**, 313 (1998).
[68]N. M. Plakida, arXiv:1110.6715 [cond-mat.str.-el] (unpublished).
[69]A. J. Millis, H. Monien, and D. Pines, Phys. Rev. B **42**, 167 (1990).
[70]P. Monthoux and D. Pines, Phys. Rev. B **49**, 4261 (1994).
[71]B. P. Stojković and D. Pines, Phys. Rev. B **56**, 11931 (1997).
[72]B. Arfi, Phys. Rev. B **45**, 2352 (1992).
[73]T. Das, R. S. Markiewicz, and A. Bansil, Phys. Rev. B **81**, 174504 (2010).
[74]N. M. Plakida, J. Phys. Soc. Jpn. **65**, 3964 (1996).
[75]S. Hüfner, M. A. Hossain, A. Damascelli, and G. A. Sawatzky, Rep. Prog. Phys. **71**, 062501 (2008).
[76]M. Jarrell, J. K. Freericks, and Th. Pruschke, Phys. Rev. B **51**, 11704 (1995).
[77]A. Toschi, M. Capone, M. Ortolani, P. Calvani, S. Lupi, and C. Castellani, Phys. Rev. Lett. **95**, 097002 (2005).
[78]J. P. Carbotte, E. Schachinger, and J. Hwang, Phys. Rev. B **71**, 054506 (2005).
[79]E. Schachinger, D. Neuber, and J. P. Carbotte, Phys. Rev. B **73**, 184507 (2006).
[80]S. G. Sharapov and J. P. Carbotte, Phys. Rev. B **72**, 134506 (2005).